



# Fractional Order Modeling of PWR Pressurizer Dynamics and Fractional Order Nonlinear $H_{\infty}$ Controllers Design in LabVIEW

Arshad H. Malik<sup>1\*</sup>, Aftab A. Memon<sup>2</sup>, Feroza Arshad<sup>3</sup>, and Mehwish Shaikh<sup>4</sup>

<sup>1</sup>Department of Basic Training, Chashma Centre of Nuclear Training,  
Pakistan Atomic Energy Commission, Chashma, Pakistan

<sup>2</sup>Department of Telecommunication Engineering, Mehran University of Engineering and  
Technology, Jamshoro, Pakistan

<sup>3</sup>Department of Information System, Karachi Nuclear Power Generating Station,  
Pakistan Atomic Energy Commission, Karachi, Pakistan

<sup>4</sup>Department of Software Engineering, Mehran University of Engineering and Technology,  
Jamshoro, Pakistan

**Abstract:** The novel fractional order intelligent transient dynamics and advanced fractional order nonlinear robust control synthesis scheme of the Pressurized Water Reactor (PWR) pressurizer are addressed in this research work. The Graphical User Interface (GUI) is designed for closed-loop model-based PWR pressurizer dynamical studies in LabVIEW. Based on the demand for power, the reactor power and turbine power are predicted using a fractional order backpropagation algorithm in an open loop configuration. Using turbine power and heater power as input variables, pressurizer level, pressurizer pressure and coolant average temperature as output variables, the open loop multi-input multi-output (MIMO) dynamic model of pressurizer is estimated using fractional order artificial intelligence in LabVIEW. Four fractional order robust nonlinear  $H_{\infty}$  sub-controllers are designed for charging flow, spray flow, proportional heaters power and backup heaters power. All the dynamic controller models are in fractional order nonlinear  $H_{\infty}$  framework and are designed in LabVIEW. The performance of the proposed design work is evaluated in closed loop configuration at 100 %, 75 % and 15 % in steady state conditions. Dynamic transient analysis is performed from 100 % to 90 % power reduction scenario and found satisfactory and within design limits and robust bounds.

**Keywords:** Fractional Order, Neural Estimation, PWR Pressurizer, Robust Controller, LabVIEW

## 1. INTRODUCTION

In this research work, the Pressurized Water Reactor (PWR)-type nuclear power plant of 340 MWe rating, operating in Pakistan is considered for closed-loop dynamic modeling and control design purposes. A non-equilibrium three-region analytical transient model of PWR pressurizer is developed by Baek *et al.* [1]. An analytical pressurizer model for 1a 200 MWe VVER type nuclear power plant is addressed by Sheta *et al.* [2] for simulation purposes. The dynamics of the 1200 MWe VVER pressurizer is investigated in detail using Modelica software by Rabie *et al.* [3] for

parametric studies. A 300 MWe PWR is adopted by Takasuo *et al.* [4] for the analytical modeling of the pressurizer pressure system. A nuclear codes-based approach is considered by Xu *et al.* [5] which was implemented for PWR pressurizer dynamic modeling using APROS and TRACE nuclear codes. A VVER pressurizer model is identified using the system identification technique by Varga *et al.* [6] for data-driven modeling. PWR pressurizer surge characteristics is modeled by Lin *et al.* [7] in 3D using transient analysis for the time-dependent studies. Sensitivity analysis of VVER 1000 PWR pressurizer level is performed by Groudev *et al.* [8]. PWR simulator is developed by Suryabrata *et al.* [9]

in MATLAB using linearized state space modeling for controller design purposes. A conventional permissive and interlocks-based PWR pressure control module is developed by Yu *et al.* [10] for condition-based logics developed using MATLAB. PID controller-based pressurizer pressure controller is designed by Zhang *et al.* [11] for closed loop model development for 900 MWe PWR nuclear power plant. A similar approach is adopted by Sheta *et al.* [12] for 1350 MWe PWR pressurizer pressure and level controllers using the PID algorithm. A fuzzy PID controller is designed by Victor *et al.* [13] for a PWR pressurizer for gray control synthesis and compared with PID controller performance. A fuzzy logic controller is synthesized by Victor *et al.* [14] for PWR pressurizer in detail using rule-based approach. A fuzzy PID controller is adopted by Sheta *et al.* [15] for VVER 1200 pressurizer. The fractional order PID controller is designed by Damayanti *et al.* [16] for the PWR pressurizer level controller which is different from pressure control logic. Fractional order neural transient modeling of the primary circuit of ACP1000 based nuclear power plant is carried out by Malik *et al.* [17] in LabVIEW for a generation-3 nuclear power plant. A fractional order nonlinear  $H_\infty$  controller is designed by Xue *et al.* [18] for the self-balancing system in dynamic mode. Such study is extended for advanced fractional order controllers design using artificial intelligence for PWR pressurizer dynamics. Finite-time synchronization of fractional order memristor-based neural networks with time delays are addressed by Velmurugan *et al.* [19] which is a class of fractional neural network.

In this research work, the new coupled pressurizer pressure and level dynamics are estimated using state-of-the-art fractional order intelligent neural network algorithm in LabVIEW.

Four new controllers are configured for charging flow control, spray control, proportional heaters power control and backup heaters power control using novel fractional order nonlinear  $H_\infty$  control framework using intelligent control design algorithm in most modern graphical programming environments using LabVIEW. LabVIEW has been selected as a programming platform because it has a more powerful GUI than visual basic and MATLAB. Further, LabVIEW is a totally graphical programming environment with excellent and

improved data flow and function control.

## 2. MATERIALS AND METHODS

### 2.1. PWR Pressurizer

The pressurizer is the main equipment of the reactor heat removal system in PWR and is used to regulate the pressure of the reactor coolant. The main function of the primary heat transport system is to remove heat from the reactor core to the steam generator. The primary loop consists of two loops designated as loop-A and loop-B. In the primary loop, there are two steam generators, one pressurizer, one reactor coolant pump and a piping structure. There are two loops in the primary system to accommodate two steam generators. So, the single loop cannot be used to achieve the dynamics of two steam generators.

The reactor coolant pressure is controlled by the pressurizer to prevent departure from nucleate boiling (DNB), which has adverse effects on heat transfer. Single pressurizer is used for two loop primary system so that the system pressure can be maintained at a single pressure else more pressurizers will try to create differential pressure in the primary circuit that will result in flow disturbance.

The reactor coolant pressure control is carried out by the action of electric heaters and spray valves. The spray system is fed from two cold legs and is connected to the pressurizer through the spray nozzle. A small continuous spray flow is provided through the flow-regulating valve. The electric heaters are installed at the bottom head of the pressurizer. Over-pressure protection is provided by two pressurizer safety valves and two pressurizer relief valves connected to the pressurizer.

The discharge of pressurizer safety and relief valves are joined to the relief header and then routed to the pressurizer relief tank. The relief tank also collects leak-off and discharges from valves of some other systems located inside the containment. The pressurizer relief tank is blanketed by nitrogen inside and equipped with an internal spray for cooling.

The pressurizer is a vertical, cylindrical vessel

with hemispherical top and bottom heads. Electrical heaters are installed vertically in the bottom head. The surge line nozzle is located in the center of the bottom head, at the lowest point of the pressurizer. This surge line is connected at its other end to the Loop B hot leg. A retaining screen is located just above the inlet of the surge line to mix the surged water with the water contained in the pressurizer and to prevent the entrance of foreign matters into the reactor coolant system.

The top head receives the spray line nozzle and the pressurizer relief and safety valve nozzles. Spraying of cold water from the cold legs of the reactor coolant piping is achieved in a fog state through a spray nozzle located at the end of the spray line inside the pressurizer. Thus the spraying can be better mixed with the saturated steam in the pressurizer to achieve a better cooling effect and reduce the pressure of the pressurizer.

The pressurizer is used to accommodate positive and negative surges caused by load transient. During an insurge, the spray system condenses steam in the pressurizer to prevent the pressurizer pressure from reaching the set point of the relief valve. During an out surge, the flashing of water and generation of steam by automatic actuation of the electrical heaters keep the pressure of the pressurizer above low-pressure reactor trip set point. The pressurizer is designed to accommodate in and out surges caused by load transients. It provides a point in the reactor coolant system (SRC) system where liquid and vapor can be maintained in equilibrium under saturated conditions for pressure control purposes. Since there are continuous process pressure fluctuations in the reactor coolant system. So, spray flow is continuous which provides minor flow while heater logic is used to compensate spray flow.

## 2.2 Pressurizer Pressure and Level Control System

The pressurizer spray lines and valves are designed to provide the necessary spray rate selected to prevent the pressurizer pressure from reaching the opening set point of the pressurizer relief valve following a step-load reduction of the 10% of full load. The pressurizer spray is controlled by two automatically controlled, air-operated downstream of the spray valves to the spray line. The auxiliary

spray path is used to provide auxiliary spray during reactor cool down when the reactor coolant pumps are out of service.

The pressurizer is equipped with 90 electric heaters in which 30 elements are proportional heaters, while the other 60 elements are reserved heaters. The heaters are direct immersion straight tubular sheath type. The tubular sheath is sealed at its upper end by a welded plug and at its lower end by a connection socket which remains leak proof even in the event of sheath failure. The heater, made of nickel-chrome alloy, is isolated from the sheath by compacted, magnesium oxide. The pressurizer electrical heater capacity is designed to heat the pressurizer water at the average rate of 45 °C / h taking into account the continuous spray flow rate. The conventional pressurizer pressure and level control system consist of modules which are designed based pressurizer pressure and level interlocks [1].

## 2.3 Fractional Order Pressurizer Control System

The fractional order pressurizer closed-loop control system consists of fractional order pressure intelligent modeling and four coupled fractional order controllers. Fractional order pressurizer intelligent modeling consists of coupled pressure and level dynamics of pressurizer while four fractional order advanced controllers are designed for charging flow control, pressurizer spray control, proportional heaters power control and back-up heaters power control as in Figure 1.

Total heater power is the sum of proportional heaters power and backup heaters power. Proportional heaters work all the time in minor transients of spray flow while backup heaters work when 100 % proportional heater are used in transients [1].

## 2.4 Fractional Order Pressurizer Intelligent Modeling

### 2.4.1 Selection of Input and Output Variables

One pair of demanded power and turbine power is used as the first single input single output fractional-order neural network (FO-SISO-ANN1) while the second pair of demanded power and reactor power

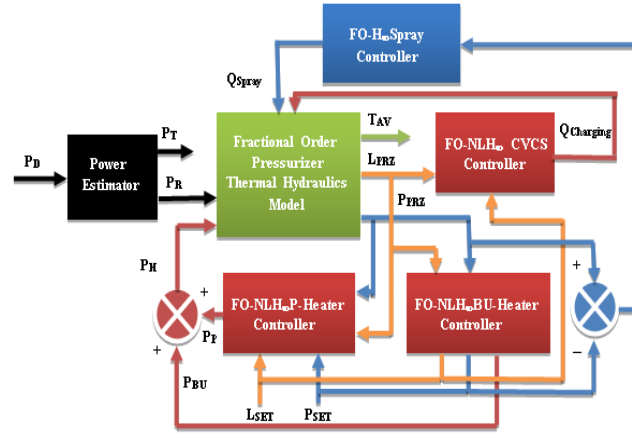


Fig. 1. Proposed closed loop pressurizer pressure and level control system.

is used as the second single input single output fractional-order neural network (FO-SISO-ANN2). Third multi-input multi-output fractional-order neural network (FO-MIMO-ANN3) is comprised of reactor power and heater power as inputs while coolant average temperature, pressurizer pressure and pressurizer level as outputs.

### 2.4.2 Choice of Modeling Algorithm

In this research work, all three FO-SISO-ANN1, FO-SISO-ANN2 and FO-MIMO-ANN3 are modeled using the model developed in [17] for the new and modified formulation of the proposed work.

The output of FO-SISO-ANN1 is given as:

$$\hat{P}_T(t_k) = \Delta_k^\alpha f \left[ \sum_{n_q=1}^q w_{nq,nr}^{[1]} \Delta_k^\alpha f \left( \sum_{n_p=1}^1 w_{np,nq} P_{Dn_p}^{[1]}(k) \right) \right]$$

The output of FO-SISO-ANN2 is given as:

$$\hat{P}_R(t_k) = \Delta_k^\alpha f \left[ \sum_{n_q=1}^q w_{nq,nr}^{[1]} \Delta_k^\alpha f \left( \sum_{n_p=1}^1 w_{np,nq} P_{Dn_p}^{[1]}(k) \right) \right]$$

The output of FO-MIMO-ANN3 is given as:

$$\hat{Y}_{n_r}(t_k) = \Delta_k^\alpha f \left[ \sum_{n_q=1}^q w_{nq,nr}^i \Delta_k^\alpha f \left( \sum_{n_p=1}^4 w_{np,nq} u_{n_p}^i(k) \right) \right]$$

Where symbols having their usual meanings.

## 2.5 Fractional Order Nonlinear Robust Controller

### 2.5.1 Problem Formulation

Since spray and heater are highly disturbing parameters. So, a robust  $H_\infty$  framework is required for the pressurizer circuit.

If  $t = kT_s$  where  $T_s$  is the sample time and assuming  $v = 1, 2, 3, \dots, n$ ,  $z = 1, 2, 3, \dots, n$  such that  $z_v, A_z(\cdot), y_c(t), u_v(t), d_v(t)$  and  $w_{vz}$  are positive constants, the nonlinear activation function of  $v$ -th neuron, controlled system output, control input of  $v$ -th neuron, unknown disturbance and memristive weights respectively, then controlled output of closed-loop control system in the continuous time domain is given as using [19]:

$$D_t^\alpha y_c(t) = -z_v y_c^v(t) + \sum_{z=1}^n w_{vz} y_c^z(t) A_z(y_c^z(t)) + u_v(t) \quad (4)$$

The performance index of fractional order nonlinear robust controller is given as:

$$\|T_{NLH_\infty}(s)\|_\infty < \gamma = \left( \frac{\sum_{v=1}^n e_v(t)^2}{\sum_{v=1}^n d_v(t)^2} \right) \quad (5)$$

Since there are four  $H_\infty$  controllers for the pressurizer circuit, so there are four control design parameters ( $y_1, y_2, y_3$  and  $y_4$ ).

2.5.2 Configuration of Sub-Controllers

The charging flow controller is configured using pressurizer level dynamics. The spray controller is configured using pressurizer pressure dynamics. The proportional heaters power controller and backup heaters power controller are configured using pressurizer pressure and level dynamics using formulation developed in equations (4) and (5). All the four controllers work together in a parallel computing scheme using artificial intelligence.

3. RESULTS AND DISCUSSION

3.1 Development of Pressurizer and Control Flow Models in LabVIEW

All the modeling, analysis and simulation work is carried out in LabVIEW. The two-loop primary circuit process flow is shown in Figure 2. The PWR pressurizer pressure and level control flow diagram is shown in Figure 3.

3.2 Steady State and Transient Analysis of Closed Loop Simulation Model in LabVIEW

The dynamic closed loop of the pressurizer system is initialized at 100 % demanded power. In response to the initialization of the model and controllers at 100 % power, trends of various parameters of interest are simulated and tested at 100 % power condition of the plant as shown in Figure 5.

Now, the reactor power is reduced from

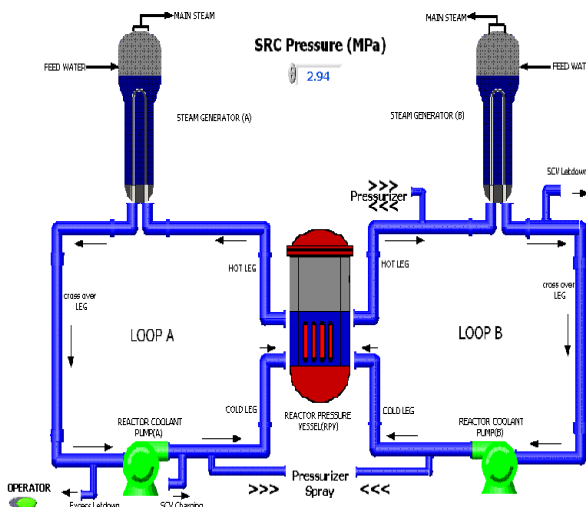


Fig. 2. Two loop primary circuit design of PWR in LabVIEW

100 % power level to 75 % power level and trends of various parameters of interest are simulated for this power reduction transient condition and tested at 100% power condition as shown in Figure 6 and Figure 7.

The simulation shows that backup heaters are turned on in this simulation experiment as indicated by the red color.

Now, another large power transient is tested in which the reactor power is reduced from 100 % power level to 15 % power level and the simulation shows that proportional heaters are turned on in this simulation experiment as indicated by the red color as shown in Figure 8.

Now, in order to assess the parametric dynamic behavior of various parameters, the power transient is simulated, tested and visualized in which the reactor power is reduced from 100 % power level to 90 % power level and various parameters are analyzed on different time intervals as shown in Figure 8 to Figure 14.

In Figure 12, pressure flow is shown but in this scenario, it is very small and near zero on the fractional scale. However, it is clear and visible in Figure 9 which shows the initiation of the spray flow transient.

Since heater power is the primary side parameter while turbine power is the secondary side parameter. So its impact is very slowly transmitted

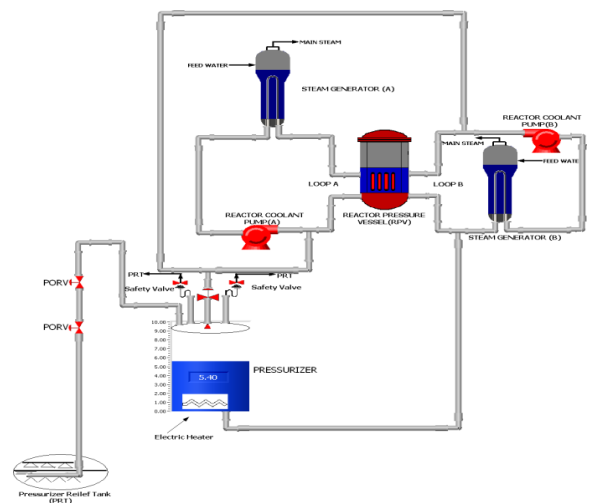


Fig. 3. Pressurizer pressure and level control system design of PWR in LabVIEW

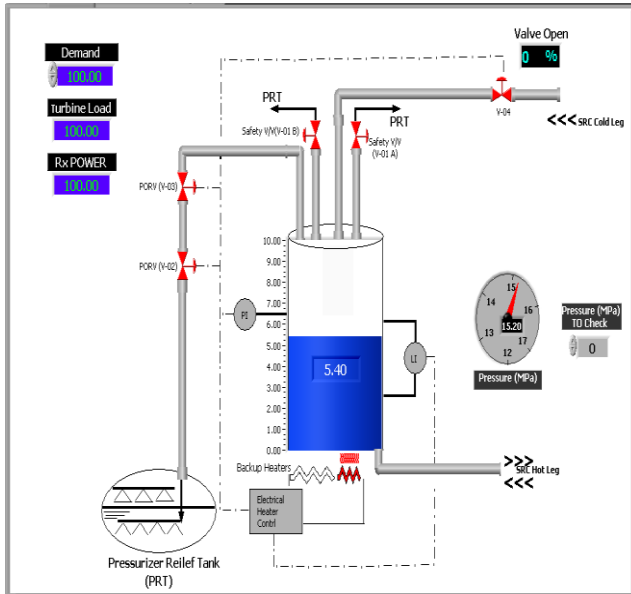


Fig. 4. Transient simulation model of pressurizer.

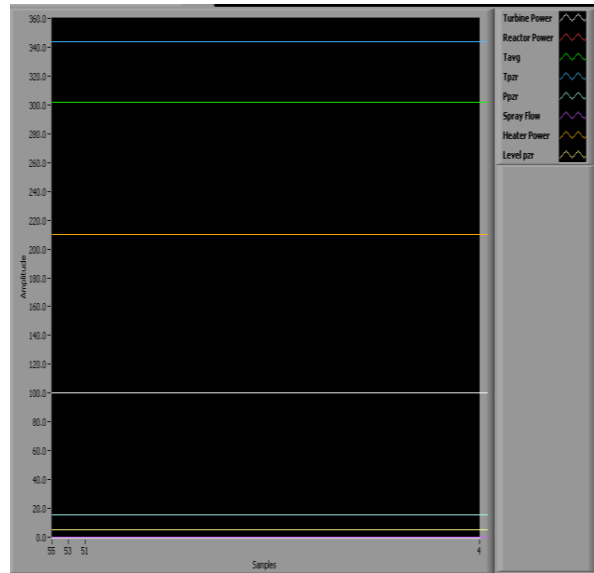


Fig. 5. Trends of pressurizer steady-state parameters at 100% steady state power

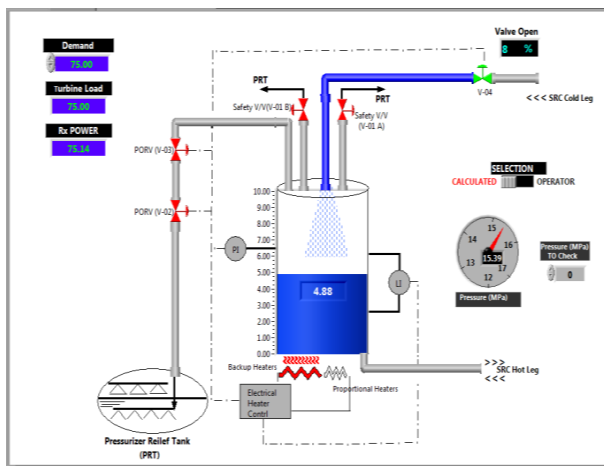


Fig. 6. Transient simulation model of pressurizer when reactor power level is reduced from 100 % to steady 75 %.

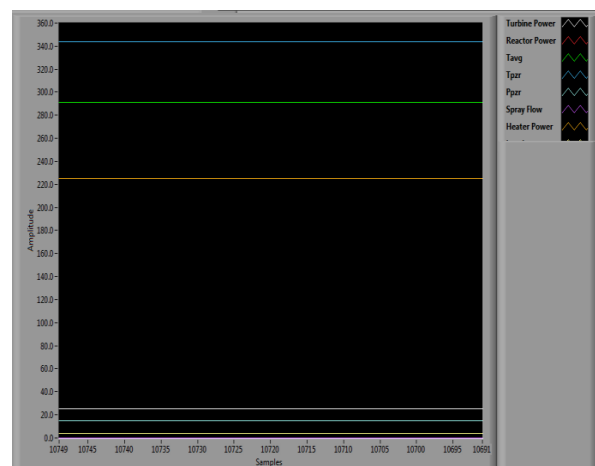


Fig. 7. Trends of pressurizer steady state parameters at 25% steady state power.

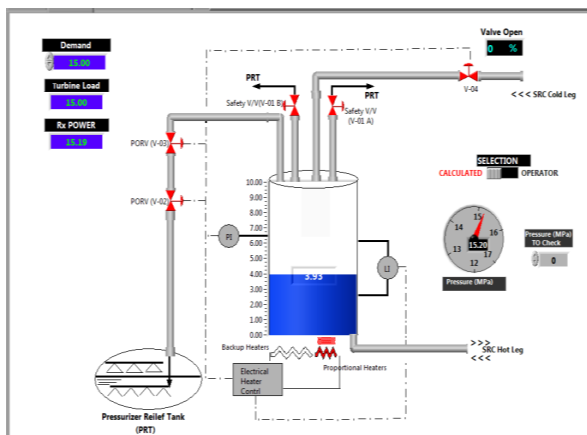


Fig. 8. Transient simulation model of pressurizer when reactor power level is reduced from 100 % to steady 15 %.

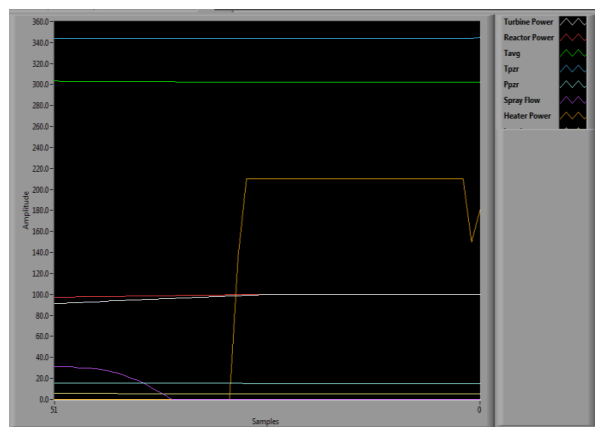


Fig. 9. Trends of pressurizer parameters from 100 % to 90 % power transient at 51<sup>st</sup> sample state.

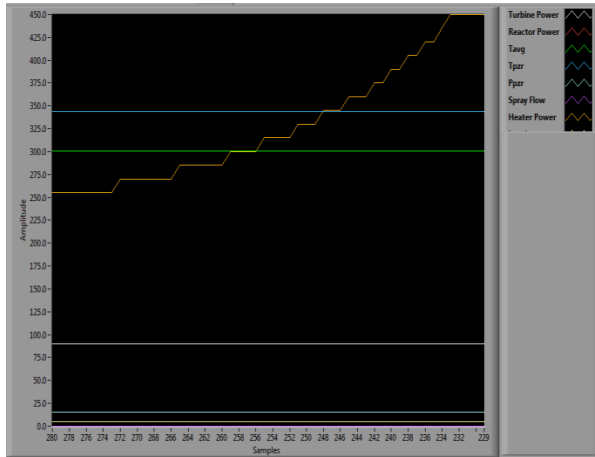


Fig. 10. Trends of pressurizer parameters from 100 % to 90 % power transient at 114<sup>th</sup> sample state.

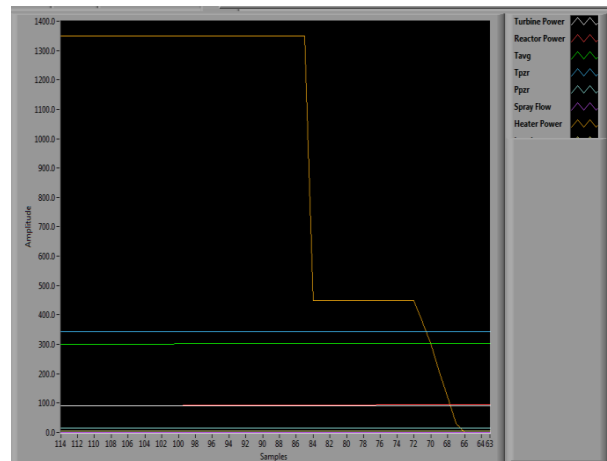


Fig. 11. Trends of pressurizer parameters from 100 % to 90 % power transient at 180<sup>th</sup> sample state

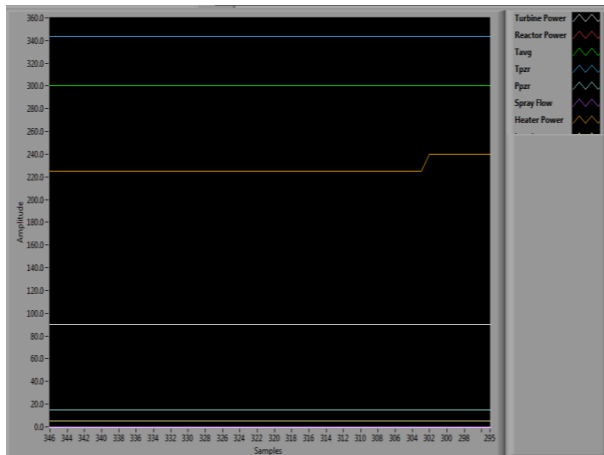


Fig. 12. Trends of pressurizer parameters from 100 % to 90 % power transient at 280<sup>th</sup> sample state

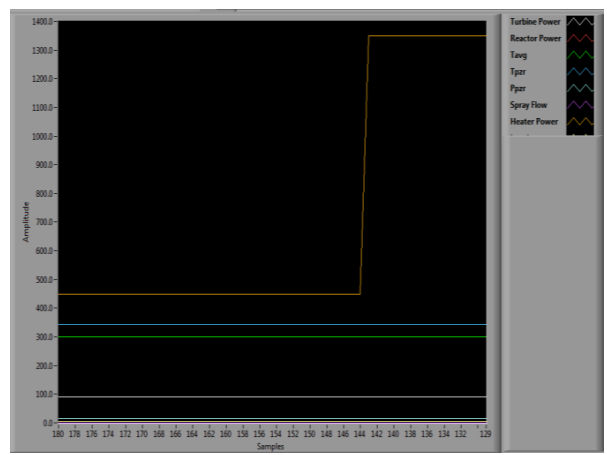


Fig. 13. Trends of pressurizer parameters from 100 % to 90 % power transient at 346<sup>th</sup> sample state.

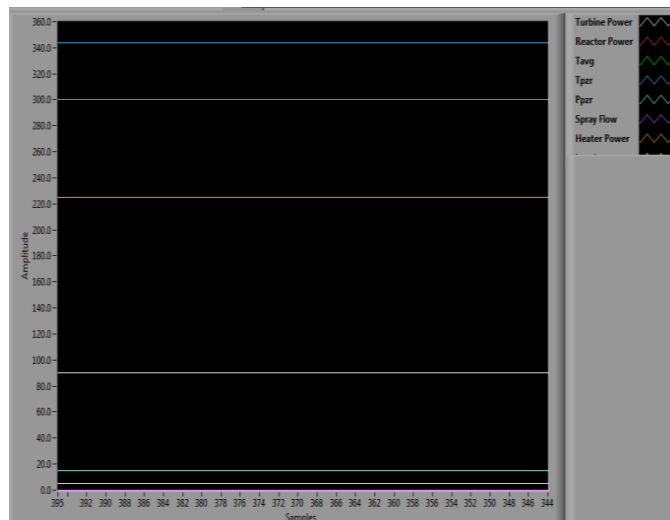


Fig. 14. Trends of pressurizer parameters from 100 % to 90 % power transient at 395<sup>th</sup> sample state

to the secondary side with process and system delay. However, in Figure 9, it is obvious that as heaters are turned OFF at the 25<sup>th</sup> sample, turbine power starts decreasing. Hence, this relationship is quite clear at the 25<sup>th</sup> sample of time.

Since FO MIMO is the combination of the FO SISO algorithm. Since the FO MIMO is a multivariable algorithm while FO SISO is a single variable algorithm, so the results are different.

This simulation experiment proves that dynamic transient analysis is excellent in tracking and parameters are settled after the transient is die out hence its performance is proved robust.

#### 4. CONCLUSION

The nonlinear dynamics of the PWR pressurizer of 340 MWe PWR have been predicted in a graphical programming environment in LabVIEW. The model parameters have been estimated in a nonlinear open-loop MIMO framework. A graphical user interface has been developed for variable transfer and parametric display in LabVIEW. Four controllers have been synthesized for charging flow control, spray flow control, proportional heaters power control and backup heaters power control. All the four controllers have been configured with a pressurizer nonlinear dynamic model in fractional order nonlinear robust stabilizing  $H_\infty$  framework. Controllers have been optimized in LabVIEW. The closed-loop performance of the PWR pressurizer has been studied in steady state and transient conditions. The fast convergence of parameters in transient conditions stabilizing at 90% demanded and turbine power proves that the robust performance of the proposed scheme is achieved. The presented design scheme can be used for other PWR systems and controllers and ever for different generations of PWRs in future.

#### 5. ACKNOWLEDGEMENTS

The support of the Pakistan Atomic Energy Commission, Chashma Centre of Nuclear Training and Computer Development Division of KANUPP is gratefully acknowledged.

#### 6. CONFLICT OF INTEREST

The authors declared no conflict of interest.

#### 7. REFERENCES

1. S. M. Baek, H. C. No, and I. Y. Park. A nonequilibrium three-region model for transient analysis of pressurized water reactor pressurizer. *Nuclear Technology* 74: 260-266 (1986).
2. A. A. Sheta, E. A. Ali, R. M. Fikry, S. M. Elaraby, T. A. Mahmoud, and M. I. Mahmoud. A developed analytical model for pressurizer unit in nuclear power plants. *Journal Radiation Research and Applied Sciences* 14: 179-203 (2021).
3. M. A. Rabie, A. Elshahat, and M. H. Hassan. Investigation of VVER-1200 pressurizer dynamics by adopting modelica based modeling. *Progress in Nuclear Energy* 143: 01-17 (2022).
4. E. Takasuo. Modeling of pressurizer using APROS and TRACE thermal hydraulic codes. *VTT Technical Research Centre of Finland* 2339: 108 (2006).
5. Z. B. Xu, J. Wu, Z. T. Quan, X. S. Zhang, and X. Q. Ma. Model and simulation study on pressurizer pressure system. *International Conference Electrical, Automation and Mechanical*: 404-407 (2015).
6. I. Varga, G. Szederkenvi, and K. M. Hangos. Modeling and model identification of a pressurizer at the PAKS nuclear power plant. *14<sup>th</sup> IFAC Symposium on System Identification, Newcastle, Australia* 39: 678-683 (2006).
7. J. Lin, J. Zhang, J. Shi, and D. Li. Research of PWR pressurizer insurge characteristics on three-dimensional transient modeling. *Science and Technology of Nuclear Installations* 2018: 1-13 (2018).
8. P. P. Groudev, and M. P. Pavlova. Sensitivity calculations of PRZ water level during the natural circulation test at unit 6 of Kozloduy NPP. *Progress in Nuclear Energy* 49: 130-141 (2007).
9. A. G. Suryabrata, T. Mulyana, and D. Witarayah. Pressurizer simulator. *Proceeding of International Conference on Electrical Engineering, Computer Science and Informatics, Palembang, Indonesia, Advances in Difference Equations*: 46-51 (2015).
10. M. Yu, X. Zhao, Y. Niu, and P. Yang. Modeling and simulation of pressure control logic module in pressurizer of nuclear power plant. *Advanced Material Research* 860: 2409-2414 (2014).
11. G. D. Zhang, X. H. Yang, S. Y. Qiao, and Y. J. Wu. Research on pressurizer pressure control of 900 MW pressurized water reactor nuclear power plant. *Advanced Material Research* 718: 1215-1220 (2013).
12. A. A. Sheta, E. H. Ali, R. m. Filry, T. A. Mahmoud,

- S. M. El-Araby, and M. I. Mahmoud. Efficient linearized model of pressurizer system in pressurized water reactors for control purposes. *Journal of Physics* 1447: 01-12 (2019).
13. M. Victor, D. Oliveira, and J. C. S. Aleida. Modeling and control of a nuclear power plant using AI techniques. *International Nuclear Atlantic Conference, Brazil* 2013: 01-15 (2013).
  14. M. Victor, D. Oliveira, and J. C. S. Aleida. Fuzzy control applied to nuclear power plant pressurizer system. *International Nuclear Atlantic Conference, Brazil* 2011: 01-15 (2011).
  15. A. A. Sheta, E. H. Ali, R. m. Filry, T. A. Mahmoud, S. M. El-Araby, and M. I. Mahmoud. Intelligent control for pressurizer system in nuclear power. *Journal of Physics* 2128: 01-13 (2021).
  16. R. Damayanti, A. Halim, and S. Nakhri. Control of air pressurizer levels on pressurized water reactor with fractional order PID control system. *Journal of Physical Science and Engineering* 05: 71-82 (2020).
  17. A. H. Malik, A. A. Memon, and F. Arshad. Fractional order neural transient modeling of primary circuit of ACP1000 based nuclear power plant in LabVIEW. *Proceedings of Pakistan Academy of Sciences-A, Physical and Computational Sciences* 58: 17-26 (2021).
  18. H. Xue, Q. Fang, J. Zhong, and Z. Shao.  $H_\infty$  Time-delayed fractional order adaptive sliding mode control for two-wheel self-balancing vehicles. *Computational Intelligence and Neuroscience* 2020: 01-12 (2020).
  19. G. Velmurugan, R. Rakkiyappan, and J. Cao. Finite time synchronization of fractional order memristor based neural networks with time delays. *Neural Networks* 73: 36-46 (2016).

